European Journal of Chemistry

Check for updates

View Journal Online
View Article Online

Synthesis, crystal structures, substitutional and comparative structural analysis of copper diphosphates $LiNaCuP_2O_7$, $LiKCuP_2O_7$ and $Rb_{0.5}Na_{1.5}CuP_2O_7$

Ines Fitouri and Habib Boughzala *

Laboratoire de Matériaux et Cristallochimie, Faculté des Sciences de Tunis, Université de Tunis El Manar, 2092 Manar II Tunis, Tunisia
inesfitouri884@gmail.com (I.F.), habib.boughzala@ipein.rnu.tn (H.B.)

** Corresponding author at: Laboratoire de Matériaux et Cristallochimie, Faculté des Sciences de Tunis, Université de Tunis El Manar, 2092 Manar II Tunis, Tunisia. Tel: +216.98.595523 Fax: +216.72.220181 e-mail: habib.boughzala@ipein.rnu.tn (H. Boughzala).*

RESEARCH ARTICLE

10.5155/eurjchem.9.3.258-268.1762

Received: 11 June 2018
Received in revised form: 17 July 2018
Accepted: 28 July 2018
Published online: 30 September 2018
Printed: 30 September 2018

KEYWORDS

Copper
Powders
Phosphorus
X-ray diffraction
IR spectroscopy
Single crystal X-ray structure

ABSTRACT

The title compounds are members of the M_2O-CuO-P_2O_5 system (M = Li, Na, K and Rb), where the lithium, sodium, potassium, rubidium and cesium phases have already been structurally characterized. The studied diphosphates $LiNaCuP_2O_7$, $LiKCuP_2O_7$ and $Rb_{0.5}Na_{1.5}CuP_2O_7$ belong to a large family of materials of general formula, $MM'CuP_2O_7$ (M, M' = Monovalent cation) where the elements M and M' ionic radii are decisive in the structural type determination. They were synthesized by solid-state reactions. The X-ray structural analysis show that these compounds crystallize in the $P2_1/n$ monoclinic lattice where the CuO_5 pyramidal square are linked to nearly eclipsed P_2O_7 groups by corner sharing to build up corrugated layers $[CuP_2O_7]^{2-}$ extending perpendicularly to [010]. The Li^+, Na^+, K^+ and Rb^+ cations reside in the interlayer space and in cavities delimited by the anionic network. In this study, the synthesis, the structure, the powder diffraction, the infrared spectroscopy, the thermal analysis (DTA/TGA) and a structural comparison are presented. The structural models were validated by Bond Valence-Sum (BVS) and charge distribution (CHARDI) analysis.

Cite this: *Eur. J. Chem.* **2018**, *9(3)*, 258-268 **Journal website**: www.eurjchem.com

1. Introduction

Many structures of copper diphosphates with general formula $MM'CuP_2O_7$ (M, M' = Monovalent cation), have been widely investigated in recent years because of their storage and energy conduction properties. Owing to the low density and the high reductive power of lithium metal, a great deal of interest has been focused on the development of lithium batteries as power source for portables devices or electric vehicles [1,2]. Indeed, in order to improve their ionic behavior, we attempted to partially replace the sodium and potassium cations in α-$Na_2CuP_2O_7$ [3] and $K_2CuP_2O_7$ [4] by smaller lithium cations. This substitution can be of interest for ionic conduction properties such as in rechargeable alkali batteries [5]. Currently, the increasing cost and the high toxicity of heavy metal based batteries encourage the pursuit of the Li-ion alternative. Thanks to environmental friendliness and natural abundance of sodium resources [6], Na-ion batteries are actually under intensive investigation.

The Cu^{2+} ion coordination flexibility, moving between the square pyramidal and the trigonal bipyramid, is able to modulate the phosphate anionic framework and incite to use copper to synthesize new materials.

2. Experimental

2.1. Synthesis and crystallization

The synthesis of the studied compounds was carried out starting with the adequate reagent mixed accordingly to the indicated relative proportions in Table 1. The mixtures were finely ground and heated in a porcelain crucible up to 623 K for 12 h to eliminate volatile components. The temperature was then increased to 873 K for $LiNaCuP_2O_7$, $LiKCuP_2O_7$ and 823 K for $Rb_{0.5}Na_{1.5}CuP_2O_7$ reaching the respective melting points and held for 15 days. The samples were slowly cooled (5 K/day) to 500 K and finally allowed to cool radiatively to room temperature. The products were washed with water and rinsed with a 0.5 M aqueous solution of HCl. Only one type of regular light-blue prismatic crystals was observed for each compound. The obtained crystals were ground and checked by powder X-ray diffraction. Rietveld analysis with the program TOPAS 4.2 [7] revealed a single-phase product of $LiNaCuP_2O_7$, $LiKCuP_2O_7$ and $Rb_{0.5}Na_{1.5}CuP_2O_7$. During the synthesis, no solid solution is observed in spite of the several attempts using different initial proportions.

http://dx.doi.org/10.5155/eurjchem.9.3.258-268.1762

Table 1. Reaction mixtures made for each compound.

Compounds	Reagents	Proportion
$LiNaCuP_2O_7$	LiH_2PO_4 / NaH_2PO_4 / CuO	1:1:2:2
$LiKCuP_2O_7$	LiH_2PO_4 / KH_2PO_4 / CuO	1:1:2:2
$Rb_{0.5}Na_{1.5}CuP_2O_7$	Rb_2CO_3 / NaH_2PO_4 /CuO	2:1:1:2

Table 2. Crystallographic data and refinement parameters for compounds $LiNaCuP_2O_7$, $LiKCuP_2O_7$ and $Rb_{0.5}Na_{1.5}CuP_2O_7$.

Crystal data			
Formula	$LiNaCuP_2O_7$	$LiKCuP_2O_7$	$Rb_{0.5}Na_{1.5}CuP_2O_7$
Crystal system	Monoclinic	Monoclinic	Monoclinic
Space group	$P2_1/n$	$P2_1/n$	$P2_1/n$
a (Å)	4.988(2)	5.066(1)	7.817(2)
b (Å)	13.598(4)	14.180(2)	9.806(3)
c (Å)	8.294(2)	8.473(7)	8.644(3)
β (°)	97.17(4)	90.189(1)	104.48(2)
Unit-cell volume (Å^3)	562.1(3)	608.7(5)	641.6(3)
Z	4	4	4
Calculated density (g/cm^3)	3.160	3.094	3.820
Absorption coefficient (mm^{-1})	5.262	4.784	11.57
Crystal size (mm)	0.32×0.09×0.13	0.16×0.09×0.13	0.11×0.06×0.13
Data collection			
Temperature	398 K	398 K	398 K
Radiation, wavelength (Å)	MoK$_\alpha$, 0.71073		
F(000)	516	548	696
θ_{max} (°)	27	27	27
h, *k*, *l* ranges	-6→5, -2→17, -10→10	-6→5, -1→18, -10→10	-9→3, -1→12, -11→11
Measured reflections	2715	2765	2199
Independent reflections	1230	1323	1393
Reflections with I > 2σ(I)	1156	1201	1181
Refinement			
Refinement method	Full-matrix least-squares on F^2	Full-matrix least-squares on F^2	Full-matrix least-squares on F^2
R1(F), wR2(F^2)	1.9%, 5.9%	1.9%, 5.3%	2.8%, 7.4%
No. of refined parameters	112	112	116
GooF	1.12	1.00	1.08
(Δ/σ)max	< 0.001	< 0.001	< 0.001
$\Delta\varrho_{min}$, $\Delta\varrho_{max}$ (e.Å^{-3})	0.86, -1.29	0.44, -0.36	0.69, -1.08

2.2. X-ray structure determination

A light blue single crystal has been selected for X-ray diffraction analysis from each preparation. Data collection was performed on an Enraf-Nonius CAD-4 diffractometer, operating at 298 K with (MoK$_\alpha$ radiation, λ = 0.71069 Å). An empirical ψ-scan absorption correction was applied in all of the three cases. The structures have been solved by direct methods using SHELXS-2014 software [8] and refined by least-square full-matrix based on F^2 using SHELXL-2014 [9] and SHELXLe [10] software. A summary of the crystallographic data and structural determination for $LiNaCuP_2O_7$, $LiKCuP_2O_7$ and $Rb_{0.5}Na_{1.5}CuP_2O_7$ is provided in Table 2. The final reduced atomic coordinates, the equivalent thermal factors and the refined partial occupancies are listed in Table 3. The geometrical characteristics are detailed in Tables 4 and 5. The crystallographic data are deposit in the ICSD database [11] and can be retrieved using the respective Collection Code 433889 for $LiKCuP_2O_7$, 433890 for $LiNaCuP_2O_7$ and 434654 for $Rb_{0.5}Na_{1.5}CuP_2O_7$.

The free variable restraint (SUMP) was required to restrain the sum of the monovalent cations occupation factors accordingly to the electro neutrality of the cell content. It's worthy to note that for $LiNaCuP_2O_7$ and $LiKCuP_2O_7$ the same cationic site 1 is preferred by the lithium and the site 2 is fully occupied by the sodium and the potassium respectively as it can be seen in Table 3. After minor alignment of the atomic coordinates in $NaKCuP_2O_7$ [12] particularly for O6 an O7, selected valance angles are summarized in Table 5.

The structural models are validated by the two structural tools, Bond Valence Sum (BVS) [13,14] and Charge Distribution analysis (CD) [15,16]. Both BVS and CD show expected valences (V) and charges (Q) of all the cation sites. The structural model is thus validated, as shown by the dispersion factor measuring the computed charges (Q) deviation in respect to the formal oxidation numbers. The Bond Valence computation and Charge Distribution analysis are summarized in Table 6.

2.3. Infrared spectroscopy

The infrared (IR) transmission spectra of the compounds $LiNaCuP_2O_7$ and $LiKCuP_2O_7$ were studied using the Perkin-Elmer spectrophotometer in the range of 1400-400 cm^{-1} wavenumbers containing the most significant solid state absorption bands. The samples were ground with 98% weight KBr and pressed (10 bar) into 10 mm diameter discs. The IR spectra of these two compounds presented in Figure 1 exhibit high similarity. The typical frequency ranges corresponding to symmetric (υ_s) and asymmetric (ν_{as}) P-O-P vibrational modes of the P_2O_7 group are centered at 773/914 cm^{-1} for the compound $LiNaCuP_2O_7$ and 775/908 cm^{-1} for $LiKCuP_2O_7$. The O-P-O bending and P-O stretching vibrational frequencies associated with the PO_4 are shown in multiple bands in the 408-604 and 978-1044 cm^{-1} range, respectively as shown in Table 7. To draw a parallel between the observed spectra of the tow compounds, the noted frequency shift towards the low frequencies for the bands associated to the symmetric deformation mode δ (O-P-O) and the asymmetric elongation mode ν_{as} (P-O-P) can be explained by the sodium substitution by a heavier cation, the potassium.

2.4. Powder diffraction

Using the structural data obtained by single-crystal diffraction, the calculated powder X-ray pattern can be obtained using the Diamond 3 [17] program. On the other hand, the observed X-ray patterns were registered on a Bruker D8 Advance diffractometer using the Kα1/α2 Copper radiation. The superposition of the observed and calculated raw diffraction of every compound reveals few weak unindexed Bragg pics and confirms the purity of the three synthesized phases.

Table 3. Coordinates and isotropic displacement parameters (Å²) of atoms in the crystal structure of $LiNaCuP_2O_7$, $LiKCuP_2O_7$ and $Rb_{0.5}Na_{1.5}CuP_2O_7$.

Atom	*x*	*y*	*z*	$U_{eq} = (1/3)\Sigma_i\Sigma_j U_{ij}a_i^*a_j^*a_i.a_j$	Occupancy
$LiNaCuP_2O_7$					
Li1	0.2398(8)	0.3018(3)	0.1573(5)	0.0154(15)	1.02(2)
Na1	0.2398(8)	0.3018(3)	0.1573(5)	0.0154(15)	0.03(2)
Li2	0.7691(2)	0.38605(8)	0.37307(2)	0.0175(4)	0.02(5)
Na2	0.7691(2)	0.38605(8)	0.37307(2)	0.0175(4)	1.004(5)
Cu	0.76586(5)	0.65856(2)	0.25798(3)	0.01163(13)	
P1	0.27162(2)	0.53003(5)	0.25517(6)	0.00830(15)	
P2	0.26202(2)	0.68581(4)	0.03920(6)	0.00685(15)	
O1	0.1804(4)	0.42598(2)	0.2511(2)	0.0153(4)	
O2	0.5623(3)	0.54255(2)	0.3156(2)	0.0129(3)	
O3	0.0897(3)	0.59955(2)	0.34668(2)	0.0115(3)	
O4	0.2614(3)	0.56959(2)	0.06942(2)	0.0103(3)	
O5	0.3691(3)	0.70280(2)	−0.12657(2)	0.0101(3)	
O6	−0.0249(3)	0.72131(2)	0.05316(2)	0.0105(3)	
O7	0.4493(3)	0.72874(2)	0.17198(2)	0.0091(3)	
$LiKCuP_2O_7$					
Li1	0.2548(8)	0.3064(3)	0.1519(4)	0.0159(14)	1.02(2)
K1	0.2548(8)	0.3064(3)	0.1519(4)	0.0159(14)	0.02(2)
Li2	0.75511(2)	0.39822(3)	0.38239(6)	0.01542(18)	0.03(3)
K2	0.75511(2)	0.39822(3)	0.38239(6)	0.01542(18)	0.997(3)
Cu	0.73335(5)	0.65988(2)	0.23902(3)	0.01005(11)	
P1	0.25017(2)	0.53470(4)	0.23364(6)	0.00910(14)	
P2	0.24636(2)	0.69267(4)	0.03911(6)	0.00723(14)	
O1	0.2182(3)	0.43118(2)	0.2169(2)	0.0182(4)	
O2	0.5034(3)	0.56170(2)	0.31934(2)	0.0144(3)	
O3	0.0190(3)	0.58294(2)	0.31455(2)	0.0140(3)	
O4	0.2704(3)	0.58030(2)	0.05834(2)	0.0106(3)	
O5	0.3576(3)	0.71637(2)	−0.12047(2)	0.0114(3)	
O6	−0.0455(3)	0.71758(2)	0.05421(2)	0.0101(3)	
O7	0.4138(3)	0.73352(2)	0.17365(2)	0.0101(3)	
$Rb_{0.5}Na_{1.5}CuP_2O_7$					
Na1	0.4547(5)	0.5125(4)	-0.0634(5)	0.0390(11)	0 .500(1)
Na2	0.5178(2)	0.14408(2)	0.16791(2)	0.0202(4)	1.004(9)
Rb	0.5000	0.5000	0.5000	0.0683(4)	0.495(2)
Cu	0.26021(5)	0.19311(5)	0.42517(5)	0.01255(16)	
P1	-0.10218(2)	0.33386(2)	0.29638(2)	0.0120(2)	
P2	0.15248(1)	0.35656(2)	0.11215(2)	0.0097(2)	
O1	-0.1758(4)	0.4330(3)	0.3923(4)	0.0348(8)	
O2	-0.2346(4)	0.2795(4)	0.1503(3)	0.0289(8)	
O3	0.0027(4)	0.2188(3)	0.3929(3)	0.0240(7)	
O4	0.0412(3)	0.4211(3)	0.2294(3)	0.0125(5)	
O5	0.2729(4)	0.4684(3)	0.0894(3)	0.0203(6)	
O6	0.0189(3)	0.3112(3)	-0.0387(3)	0.0160(6)	
O7	0.2505(3)	0.2344(3)	0.2014(3)	0.0177(6)	

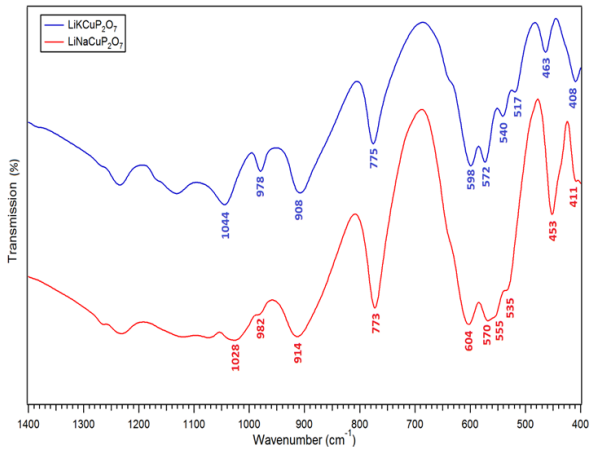

Figure 1. IR spectra of $LiNaCuP_2O_7$ diphosphates (in red) and $LiKCuP_2O_7$ (in blue).

This preliminary step is necessary to control the purity of the product, but remains limited because it is based on visual analysis and do not take care of the relative intensities of the reflections. The use of a more reliable method is crucial in a second step. In this context, a Rietveld study was carried out to identify discrepancies between the results obtained by the two techniques (single crystal and powder) and to ensure the purity of the studied material. Both GSAS [18] and TOPAS 4.2 [7] programs have been used to refine some structural parameters obtained by the single crystal diffraction investigation. The best profile fitting of the raw diffraction are plotted in Figures 2-7, respectively for the powders of $LiNaCuP_2O_7$, $LiKCuP_2O_7$ and $Rb_{0.5}Na_{1.5}CuP_2O_7$. In order to avoid obtaining incoherent values of the occupancy rates of the cations, restrictions have been applied on their respective sites, as well as a constraint respecting the electrical neutrality of the material.

Table 4. Selected bond lengths (Å) in the crystal structures of $LiNaCuP_2O_7$, $LiKCuP_2O_7$ and $Rb_{0.5}Na_{1.5}CuP_2O_7$.

$LiNaCuP_2O_7$		**$LiKCuP_2O_7$**		**$Rb_{0.5}Na_{1.5}CuP_2O_7$**	
Li-O1	1.888(5)	Li-O1	1.863(4)	Rb-O1 viii	2.984(3)
Li-O5 viii	1.978(4)	Li-O5 viii	2.008(4)	Rb-O1 ix	2.984(3)
Li-O7 ix	1.996(4)	Li-O7 ix	1.998(4)	Rb-O6 i	3.077(3)
Li-O6 vii	2.038(4)	Li-O6 vii	2.068(4)	Rb-O6 iv	3.077(3)
<Li-O>	**1.975(4)**	**<Li-O>**	**1.984(4)**	Rb-O7 i	3.232(3)
				Rb-O7 iv	3.232(3)
Na-O1 i	2.384(2)	K-O2	2.698(2)	Rb-O5	3.563(3)
Na-O2	2.405(2)	K-O1 i	2.776(2)	Rb-O5 x	3.563(3)
Na-O3 v	2.411(2)	K-O5 vi	2.808(2)	**<Rb-O>**	**3.214(3)**
Na-O5 viii	2.451(2)	K-O3 iv	2.820(3)		
Na-O7 x	2.593(2)	K-O6 ix	2.825(2)	Na1-O5 vii	2.205(4)
Na-O6 ix	2.633(2)	K-O2 iv	2.906(3)	Na1-O5	2.211(4)
<Na-O>	**2.479(2)**	K-O7 xi	2.915(2)	Na1-O3 xi	2.345(5)
		K-O3 i	2.997(2)	Na1-O3 iv	2.476(5)
Cu-O3 i	1.924(2)	K-O1	3.091(2)	Na1-O2 v	2.653(5)
Cu-O2	1.945(2)	**<K-O>**	**2.870(2)**	**<Na1-O>**	**2.378(5)**
Cu-O7	1.956(2)				
Cu-O5 ii	2.167(2)	Cu-O3 i	1.920(2)	Na2-O7	2.353(3)
Cu-O6 i	2.199(2)	Cu-O2	1.940(2)	Na2-O2 ix	2.383(3)
<Cu-O>	**2.038(2)**	Cu-O7	2.003(2)	Na2-O4 ii	2.447(3)
		Cu-O6 i	2.094(2)	Na2-O1 ii	2.530(4)
P1-O1	1.486(2)	Cu-O5 ii	2.211(2)	Na2-O6 i	2.571(3)
P1-O2	1.525(2)	**<Cu-O>**	**2.033(2)**	Na2-O1 xi	2.595(4)
P1-O3	1.531(2)			Na2-O3 xi	2.708(4)
P1-O4	1.630(2)	P1-O1	1.483(2)	**<Na2-O>**	**2.512(3)**
<P1-O>	**1.543(2)**	P1-O2	1.521(2)		
		P1-O3	1.521(2)	Cu-O2 i	1.955(3)
P2-O4	1.600(2)	P1-O4	1.623(2)	Cu-O7	1.959(3)
P2-O5	1.511(2)	**<P1-O>**	**1.537(2)**	Cu-O6 i	1.968(3)
P2-O6	1.518(2)			Cu-O3	1.978(3)
P2-O7	1.532(2)	P2-O4	1.606(2)	Cu-O5 ii	2.218(3)
<P2-O>	**1.540(2)**	P2-O5	1.504(2)	**<Cu-O>**	**2.015(3)**
		P2-O6	1.526(2)		
		P2-O7	1.532(2)	P1-O1	1.484(3)
		<P2-O>	**1.542(2)**	P1-O2	1.516(3)
				P1-O3	1.517(3)
				P1-O4	1.627(3)
				<P1-O>	**1.536(3)**
				P2-O5	1.490(3)
				P2-O6	1.519(3)
				P2-O7	1.523(3)
				P2-O4	1.620(3)
				<P2-O>	**1.538(3)**

Symmetry code: (i) $x+1, y, z$; (ii) $x+1/2, -y+3/2, z+1/2$; (iii) $-x+3/2, y+1/2, -z+1/2$; (iv) $-x+1, -y+1, -z+1$; (v) $x-1, y, z$; (vi) $-x+1, -y+1, -z$; (vii) $-x, -y+1, -z$; (viii) $-x+1/2, y+1/2, -z+1/2$; (ix) $-x+1/2, y-1/2, -z+1/2$; (x) $x-1/2, -y+1/2, z-1/2$; (xi) $-x+3/2, y-1/2, -z+1/2$; (xii) $x-1/2, -y+3/2, z-1/2$.

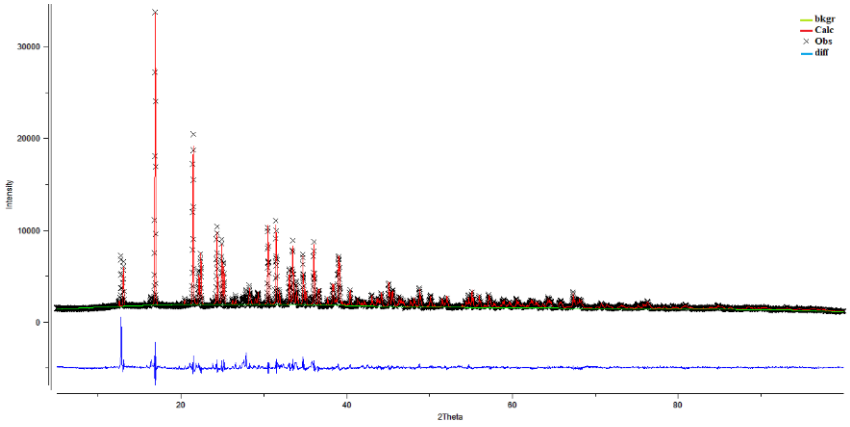

Figure 2. GSAS refinement of the $LiNaCuP_2O_7$.

If the profile and the background parameters functions are refined, the atomic coordinates and the thermal displacement parameters (obtained by the single crystal study) are fixed. Using the Table 8, a comparison of the main refined crystallographic parameters obtained by single crystal and powder diffraction can be done. Both results are close within the standard errors. Thus the crystal is representative of the powder.

2.5. Thermal analysis (DTA/TGA)

To have more information about the thermal properties of the studied compounds and particularly searching any solid state phase transition, coupled Differential Thermal Analysis (DTA) and Thermo Gravimetric Analysis (TGA) was performed on a Perkin Elmer STA6000 thermal analysis system using the polycrystalline samples of $LiKCuP_2O_7$ and $Rb_{0.5}Na_{1.5}CuP_2O_7$ in the range of 30 to 400 °C.

Table 5. Selected angles (°) in the crystal structures of $LiNaCuP_2O_7$, $LiKCuP_2O_7$ and $Rb_{0.5}Na_{1.5}CuP_2O_7$.

Bond	$LiNaCuP_2O_7$	$LiKCuP_2O_7$	$NaKCuP_2O_7$	$Rb_{0.5}Na_{1.5}CuP_2O_7$	
O3^{i}—Cu—O2	90.36(7)	85.88(7)	91.46 (8)	O2^{i}—Cu—O7	160.14(1)
O3^{i}—Cu—O7	175.44(7)	174.75(6)	160.62 (8)	O2^{i}—Cu—O6 ^{i}	94.62(1)
O2—Cu—O7	93.65(7)	89.17(7)	90.77 (7)	O7—Cu—O6 ^{i}	86.87(1)
O3^{i}—Cu—O5 ^{ii}	90.68(7)	93.35(7)	92.15 (8)	O2^{i}—Cu—O3	83.69(1)
O2—Cu—O5 ^{ii}	135.57(7)	123.43(7)	109.22 (7)	O7—Cu—O3	92.72(1)
O7—Cu—O5 ^{ii}	84.94(7)	87.91(6)	89.93 (7)	O6^{i}—Cu—O3	173.85(1)
O3^{i}—Cu—O6 ^{i}	92.36(7)	93.83(7)	91.34 (7)	O2^{i}—Cu—O5 ^{ii}	99.56(1)
O2—Cu—O6 ^{i}	140.50(7)	149.97(7)	176.22 (8)	O7—Cu—O5 ^{ii}	100.03(1)
O7—Cu—O6 ^{i}	85.93(7)	91.34(6)	87.43 (7)	O6^{i}—Cu—O5 ^{ii}	95.09(1)
O5^{ii}—Cu—O6 ^{i}	83.81(6)	86.59(7)	84.52 (7)	O3—Cu—O5 ^{ii}	91.03(1)
O1—P1—O2	113.58(1)	112.72(1)	112.67 (12)	O1—P1—O2	114.6(2)
O1—P1—O3	114.35(1)	113.83(1)	114.78 (12)	O1—P1—O3	114.35(2)
O2—P1—O3	109.99(1)	108.72(1)	108.17 (11)	O2—P1—O3	111.06(2)
O1—P1—O4	107.11(1)	108.30(9)	107.95 (11)	O1—P1—O4	104.62(2)
O2—P1—O4	105.60(1)	106.31(9)	107.13 (10)	O2—P1—O4	106.04(2)
O3—P1—O4	105.47(9)	106.51(9)	105.64 (10)	O3—P1—O4	105.12(2)
O5—P2—O6	112.78(1)	112.93(9)	113.20 (10)	O5—P2—O6	115.07(2)
O5—P2—O7	111.64(1)	112.08(1)	111.96 (10)	O5—P2—O7	113.02(2)
O6—P2—O7	112.01(1)	112.59(9)	111.49 (10)	O6—P2—O7	110.79(2)
O5—P2—O4	107.23(9)	106.51(9)	107.91 (10)	O5—P2—O4	104.53(2)
O6—P2—O4	107.13(1)	107.12(8)	105.10 (10)	O6—P2—O4	106.88(1)
O7—P2—O4	105.56(9)	104.94(9)	106.66 (10)	O7—P2—O4	105.71(1)

Symmetry code: (i) x+1, y, z; (ii) x+1/2, −y+3/2, z+1/2.

Table 6. CHARDI and BVS analysis of ions in $LiNaCuP_2O_7$, $LiKCuP_2O_7$ and $Rb_{0.5}Na_{1.5}CuP_2O_7$.

Ion	q(i).sof(i)	Q(i)	V(i).sof(i)	CN(i)	ECoN(i)	d_{ar}(i)	d_{med}(i)
$LiNaCuP_2O_7$							
Li	1.00	0.98	1.02	4	3.89	1.974	1.975
Na	1.00	0.98	1.08	6	5.80	2.479	2.479
Cu	2.00	1.95	1.98	5	4.42	2.038	2.038
P1	5.00	4.99	4.93	4	3.84	1.543	1.543
P2	5.00	5.10	4.96	4	3.93	1.540	1.540
O1	-2.00	-2.07	-1.88	3	3.00	1.919	1.913
O2	-2.00	-2.05	-1.95	3	3.00	1.959	1.958
O3	-2.00	-2.04	-2.00	3	3.00	1.955	2.207
O4	-2.00	-1.79	-2.15	2	2.99	2.316	1.339
O5	-2.00	-2.05	-1.99	4	4.00	2.702	2.027
O6	-2.00	-1.86	-1.91	3	4.00	2.097	2.097
O7	-2.00	-2.14	-2.08	4	4.00	2.019	2.202
$LiKCuP_2O_7$							
Li	1.00	0.99	0.97	4	3.79	1.984	1.984
K	1.00	0.98	1.17	9	8.52	2.547	2.870
Cu	2.00	1.95	1.97	5	4.54	2.205	2.033
P1	5.00	4.96	4.97	4	3.85	1.538	1.537
P2	5.00	5.12	4.93	4	3.92	1.542	1.542
O1	-2.00	-2.01	-1.63	4	3.79	2.304	2.040
O2	-2.00	-2.02	-2.02	4	3.93	2.315	2.053
O3	-2.00	-2.02	-2.00	4	3.90	2.266	2.146
O4	-2.00	-1.98	-2.12	2	3.00	2.326	2.081
O5	-2.00	-1.98	-1.73	4	4.00	2.132	2.132
O6	-2.00	-1.99	-1.75	4	4.00	2.128	2.128
O7	-2.00	-1.99	-1.80	4	4.00	2.111	2.286
$Rb_{0.5}Na_{1.5}CuP_2O_7$							
Rb	0.50	0.47	0.48	8	8.89	3.212	3.214
Na1	0.50	0.48	0.49	5	4.17	2.377	2.378
Na2	1.00	0.92	1.08	7	6.46	2.512	2.512
Cu	2.00	1.78	2.04	5	4.63	2.015	2.015
P1	5.00	4.7	4.98	4	3.83	1.535	1.536
P2	5.00	4.46	5.01	4	3.86	1.538	1.538
O1	-2.00	-2.39	-1.79	3	4.19	2.551	2.398
O2	-2.00	-2.14	-2.02	4	4.79	2.443	2.126
O3	-2.00	-2.03	-2.01	4	4.63	2.204	1.798
O4	-2.00	-1.88	-2.27	3	4.00	2.383	1.898
O5	-2.00	-2.14	-1.94	4	3.00	1.968	2.031
O6	-2.00	-2.47	-1.96	3	4.00	2.284	2.284
O7	-2.00	-2.46	-2.00	3	4.47	2.581	2.266

The obtained results represented in Figures 8 and 9, proof that the compounds are thermally stable and exhibit no phase transition in the explored range of temperature.

3. Results and discussion

The compounds $LiKCuP_2O_7$ and $LiNaCuP_2O_7$ exhibit the same structural arrangement with minor differences. On the other hand, the $Rb_{0.5}Na_{1.5}CuP_2O_7$ structure presents some differences that should be explained.

3.1. The structural unit

The structural units of the studied compounds are plotted on Figures 10. The PO_4 tetrahedra are almost regular, as evidenced by the bonds length and the valence angles grouped in Tables 4 and 5, respectively.

Table 7. Observed vibration frequencies (cm^{-1}) in $LiNaCuP_2O_7$ and $LiKCuP_2O_7$ and proposed assignments.

Observed frequencies		**Assignments**
$LiNaCuP_2O_7$	**$LiKCuP_2O_7$**	
773	775	ν_s (P-O-P)
914	908	ν_{as} (P-O-P)
411-604	408-598	δ (O-P-O)
982-1028	978-1044	ν (P-O)

Table 8. Cell parameters and partial cationic occupancy refinements using single crystal and powder X-ray diffraction (GSAS and TOPAS) for compounds $LiNaCuP_2O_7$, $LiKCuP_2O_7$ and $Rb_{0.5}Na_{1.5}CuP_2O_7$.

Compound	**$LiNaCuP_2O_7$**			**$LiKCuP_2O_7$**			**$Rb_{0.5}Na_{1.5}CuP_2O_7$**			
Method	**Single crystal**	**TOPAS**	**GSAS**	**Single crystal**	**TOPAS**	**GSAS**	**Single crystal**		**TOPAS**	**GSAS**
Crystal system	Monoclinic									
Space group	$P2_1/n$									
a (Å)	4.987(2)	4.992(1)	4.991(9)	5.065(1)	5.072(7)	5.070(6)	7.817(2)		7.826(1)	7.821(3)
b (Å)	13.597(4)	13.608(3)	13.606(3)	14.180(2)	14.205(2)	14.199(2)	9.806(3)		9.822(2)	9.816(3)
c (Å)	8.293(2)	8.301(2)	8.299(2)	8.473(7)	8.487(1)	8.483(1)	8.644(3)		8.662(2)	8.651(3)
β (°)	92.17(4)	92.1664(2)	92.1664(2)	90.189(1)	90.1864(1)	90.189(1)	104.48(2)		104.59(2)	104.48(1)
V ($Å^3$)	562.06(6)	563.62(3)	563.28(2)	608.7(5)	611.56(2)	610.811(1)	641.6(3)		644.430(2)	643.144(4)
Cationic	Li1 1.02(2)	0.939(2)	0.921(2)	Li1 1.02(2)	0.994(4)	0.996(4)	Na1	0.500(1)	0.498(1)	0.508(3)
sites	Na1 0.03(2)	0.061(2)	0.078(2)	K1 0.02(2)	0.006(4)	0.004(4)	Na2	1.004(9)	0.950(2)	1.015(4)
occupancies	Li2 0.02(5)	0.012(2)	0.015(2)	Li2 0.03(3)	0.003(4)	0.003(4)	Rb	0.495(2)	0.495(2)	0.502(6)
	Na2 1.004(5)	0.988(2)	0.984(2)	K2 0.997(3)	0.997(4)	0.997(4)				
Refinement										
R_{int}/R_{exp} (%)	2.70	2.26	2.25	3.10	1.63	1.63	2.40		1.51	2.48
wR/Rwp (%)	5.90	6.90	8.20	5.30	3.60	4.79	7.50		7.34	7.36
R/Rp (%)	1.90	4.20	5.42	1.90	2.60	3.41	2.80		4.63	4.65
GOOF	1.12	3.06	3.64	1.00	2.20	2.94	1.08		2.96	8.79

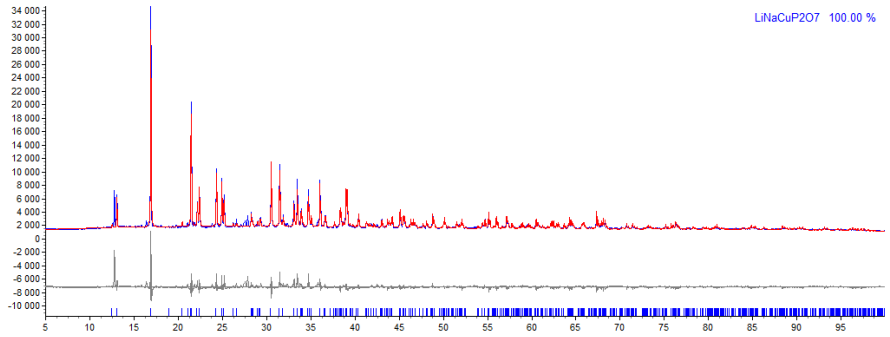

Figure 3. TOPAS refinement of the $LiNaCuP_2O_7$.

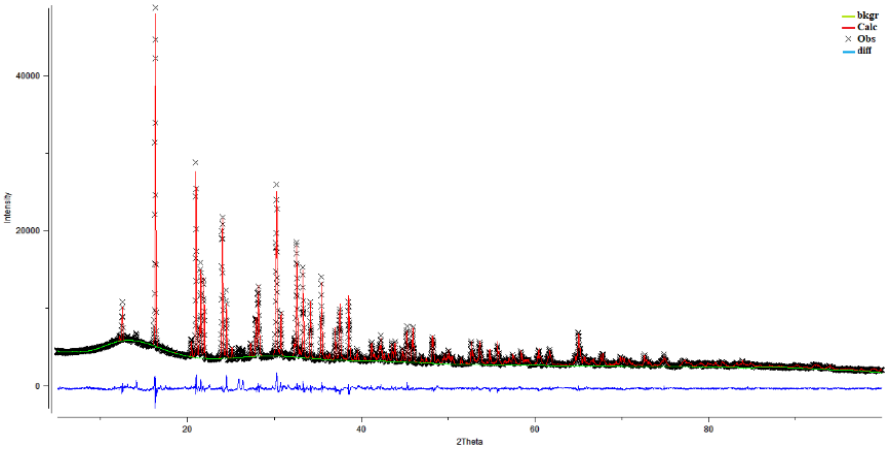

Figure 4. GSAS refinement of the $LiKCuP_2O_7$.

The phosphate polyhedra are linked by corner sharing O4 to form diphosphate groups P_2O_7 assembled with the copper pyramidal square CuO_5 by tow vertices O3 and O7. The $(CuP_2O_7)^{2-}$ units are linked together by vertices forming a corrugated anionic network.

3.2. The diphosphate group

Adopting a nearly eclipsed conformation, the O2–P2–P1–O7 dihedral angle is increasing when the alkaline atomic size decreases at the opposite to the bridging angle P2-O4-P1 as listed in Table 9.

Table 9. Values of the geometry index of the four compared diphosphates.

Compound	$LiNaCuP_2O_7$	$LiKCuP_2O_7$	$KNaCuP_2O_7$	$Rb_{0.5}Na_{1.5}CuP_2O_7$
P2-O4-P1 bridging angle (°)	118.269(9)	118.871(7)	119.01(11)	123.02(11)
O2–P2–P1–O7 dihedral angle (°)	34.71(1)	23.82(1)	15.90(1)	3.85(1)
Geometry index τ for CuO_5 polyhedron	0.58	0.41	0.26	0.22

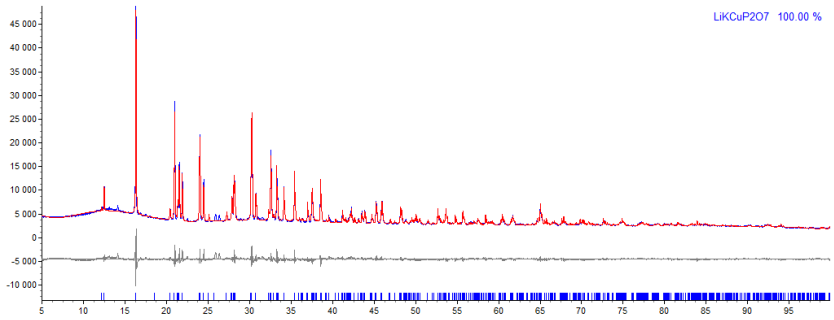

Figure 5. TOPAS refinement of the $LiKCuP_2O_7$.

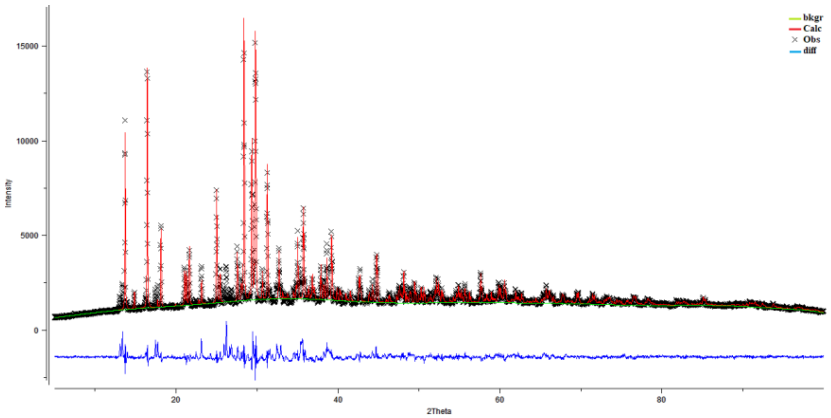

Figure 6. GSAS refinement of the $Rb_{0.5}Na_{1.5}CuP_2O_7$.

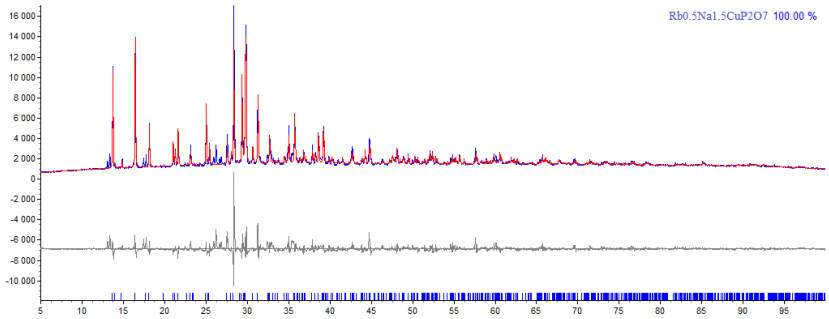

Figure 7. TOPAS refinement of the $Rb_{0.5}Na_{1.5}CuP_2O_7$.

The highest value of 123.033(7)° observed for $Rb_{0.5}Na_{1.5}CuP_2O_7$ is comparable to that for $NaCsCuP_2O_7$ [19] 122.5(1)° (the largest value is noted for β-$Rb_2CuP_2O_7$ [20] 130.3(2)°). Within the diphosphate groups the bonds P1-O4 and P2-O4 are the longest since O4 is the bridging oxygen.

Every diphosphate group is linked to three copper polyhedra leaving only one free oxygen (O1) pointing towards the empty space where the alkaline cations are lodged. The oxygen O1 charge (V(O1).sof(O1)) of -1.88, -1.63 and -1.79 in the three structures visible on Table 6 means that this oxygen is not involved in the anionic linkage and it's the first contributor in the cationic environment presenting the shortest distance Li-O, Na-O, K-O and Rb-O (see Table 4). One of the crucial differences between $LiNaCuP_2O_7$ (or $LiKCuP_2O_7$) and $Rb_{0.5}Na_{1.5}CuP_2O_7$ structures is that in the first one, this corner O1 is located in direction of the base of the CuO_5 polyhedron (Figure 10a) and in the second one it is located in the apex side (Figure 10b.).

3.3. The copper polyhedron

The crystal structures of the title compounds contain one symmetrically independent copper site surrounded by five oxygens describing a distorted square pyramidal coordination. The four oxygens of the base of the pyramid are shared with two diphosphate groups and its apex is linked to a third P_2O_7 group. Two CuO_5 polyhedra are pointing their pyramidal apex in the same direction as shown in Figure 10a. On the other hand, in $Rb_{0.5}Na_{1.5}CuP_2O_7$ the same pair of connected copper polyhedra are pointing in opposite direction (Figure 10b).

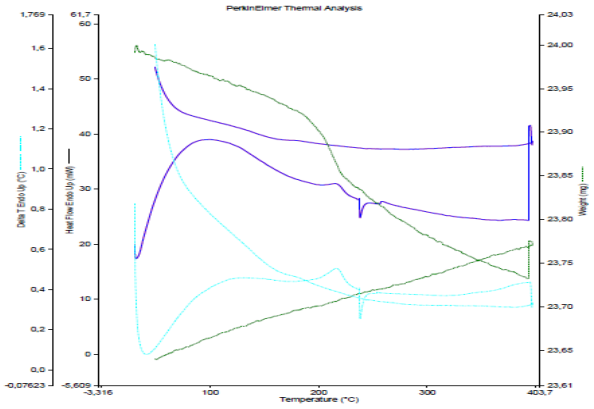

Figure 8. Thermal analysis (**DTA**/**TGA**) of $LiKCuP_2O_7$.

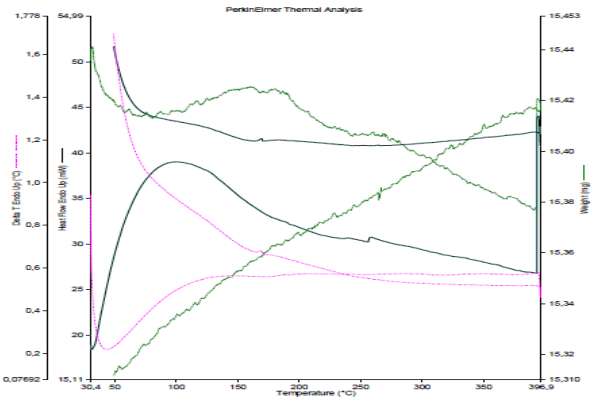

Figure 9. Thermal analysis (**DTA**/**TGA**) of $Rb_{0.5}Na_{1.5}CuP_2O_7$.

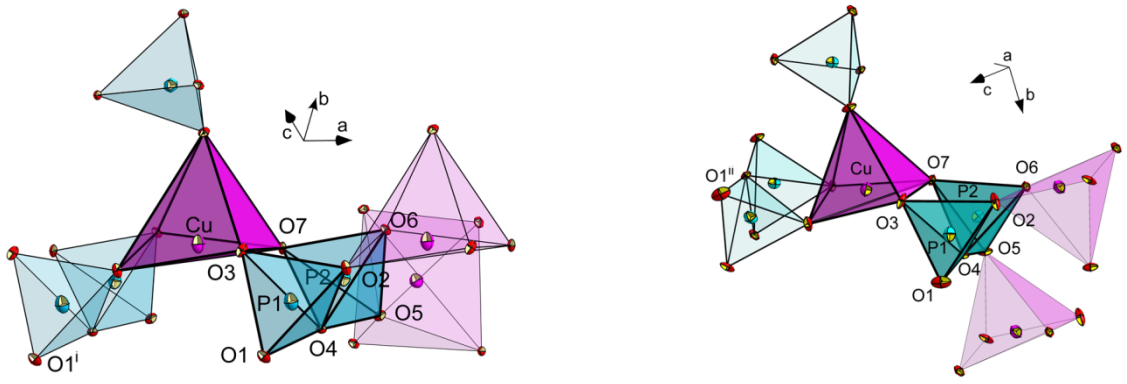

(**a**) (**b**)

Figure 10. Structural units in the crystal structures of $LiNaCuP_2O_7$ or $LiKCuP_2O_7$ (a) and $Rb_{0.5}Na_{1.5}CuP_2O_7$ (b). Symmetry code: (i): *x*-1, *y*, *z*; (ii): 0.5+*x*, 0.5-*y*, 0.5+*z*.

The described distorted pyramidal copper coordination is confirmed by the (4+1) bonds length and their angular values in Tables 4 and 5.

The τ parameter proposed by Addison [21] through the formula: $\tau = \frac{\beta - \alpha}{60} \approx -0.01667\alpha + 0.01667\beta$ was used to find the appropriate polyhedral description of copper. β and α are the two greatest valence angles of the coordination center (β > α) visible in Table 9. When τ is close to zero, the geometry is similar to square pyramidal and if τ is close to one the geometry is similar to trigonal bipyramidal. The computed values of τ parameter for the studied diphosphates and for $KNaCuP_2O_7$ [12] listed in Table 8, seem to be closely related to the monovalent cation size.

3.4. The structural packing

The 2-D structural arrangement of α-$Na_2CuP_2O_7$ is adopted by $LiNaCuP_2O_7$, $LiKCuP_2O_7$ and $KNaCuP_2O_7$. The crystal structure is build up by distorted CuO_5 square-pyramids linked to nearly eclipsed P_2O_7 groups by corners sharing leading to infinite chains running along (100) (Figure 11a). These ribbons are connected by the CuO_5 square-pyramids apex forming corrugated layers perpendicular to (010) direction (Figure 12).

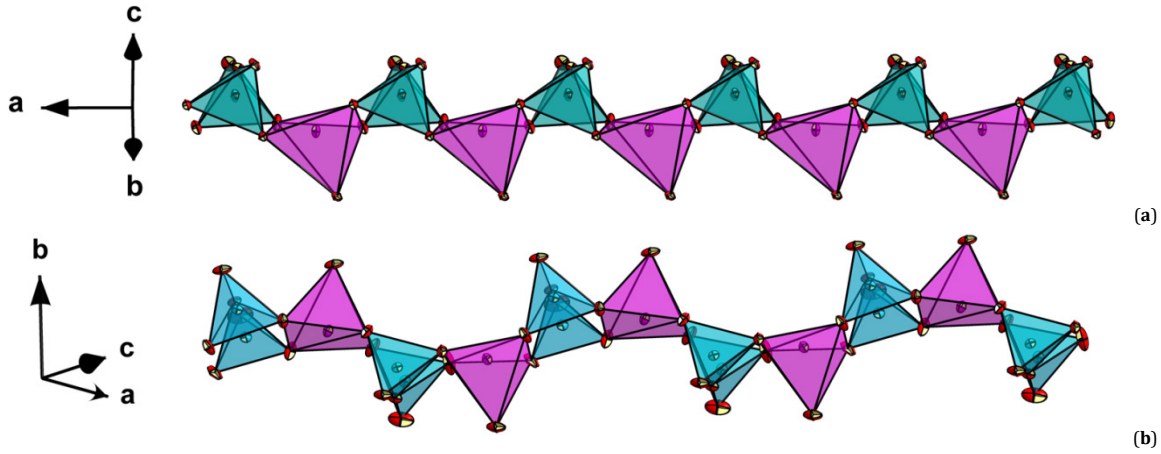

Figure 11. Different orientations of copper coordination polyhedra along the chains of the anionic network: (a) in $LiNaCuP_2O_7$ structure, (b) in $Rb_{0.5}Na_{1.5}CuP_2O_7$.

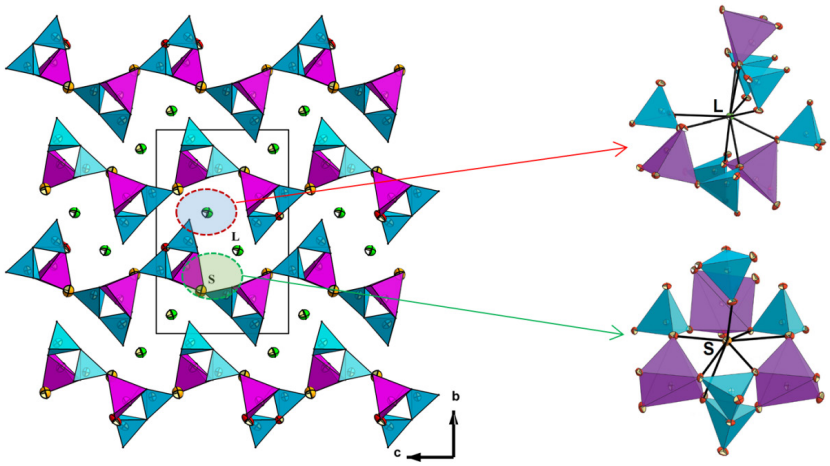

Figure 12. Projection of the $LiNaCuP_2O_7$ structural model along [100], showing the corrugated interlayer space and zoom on small (S) and large (L) cations anionic environment.

The 2-D anionic stacking leaves interlayer empty space where the largest cations (L) are lodged and ellipsoidal cavities delimited by the vertices of the P_2O_7 and CuO_5 polyhedra housing the smallest cations (S). Figure 12 represents the structure projection along (100) direction where the crystallographic sites L and S are shown.

The crystal structure of the $Rb_{0.5}Na_{1.5}CuP_2O_7$ is also build up by distorted CuO_5 square-pyramids linked to P_2O_7 groups by corners sharing leading to infinite chains running along (101) (Figure 11b). At the opposite of the $LiNaCuP_2O_7$, where the copper square pyramid polyhedra apex are oriented in a common sense in this structure they are pointing in opposite direction. Thus, larger spaces are created able to lodge the Rb^+. This double orientation leads to building undulated 2-D anionic framework and leaves empty interlayer space where and Na^+ are lodged. A structure projection is plotted on Figure 13.

3.5. The cationic sites occupancies

The main important result deduced from this study and that of $KNaCuP_2O_7$ is the identification of two kinds of cationic sites in the structure. The first, located in the interlayer space, is booked for large cations (L) and the second for smaller one (S), having an ellipsoidal shape and delimited by the anionic network. Similar results related to the compounds with general formula $A^I_3M^{III}_3(XO_4)_4$ (A^I = Alkali metal, M^{III} = Al, Cr, Fe, … X = As, P) were published by our team [22]. Nevertheless, in the structure of $Rb_{0.5}Na_{1.5}CuP_2O_7$ the interlayer space is more regular, thus the large Rb^+ cation is lodged on a special position in large intersecting channels of the anionic framework with 50% occupancy. As observed in the studied compounds, the partial cationic site occupancy is a promising structural property offering a large interlayer space where the cationic mobility is possible. Thus, they can be potential candidates for interesting energy storage and conduction behavior. The complex impedance measurements of these compounds are underwork.

3.6. The structural filiation

Based on the content of the Table 10, a comparative study can be done between the members of the alkaline copper diphosphate family. The structures of $LiNaCuP_2O_7$, $LiKCuP_2O_7$, $KNaCuP_2O_7$ [12] and $Rb_{0.5}Na_{1.5}CuP_2O_7$ are similar to that of α-$Na_2CuP_2O_7$ [3]. Nevertheless, increasing the alkali cation size seems to introduce further symmetry, indeed, the Rb^+ cation adopts a special position in the structure of $Rb_{0.5}Na_{1.5}CuP_2O_7$.

Accordingly, to the anionic 2D network topology, built up by linked $(CuP_2O_7)^{2-}$ units, the three studied compounds can be classified into the same group of selected copper diphosphates.

Table 10. Crystallographic data and topological type of the $[CuP_2O_7]^{2-}$ anionic network for copper diphosphates $MM'CuP_2O_7$ (M and M' = Monovalent metal).

Compound	Space group	*a* (Å)	*b* (Å) β (°)	*c* (Å)	Cell Volume (Å³)	Topology of the anionic network	References
Band structures							
$Li_2CuP_2O_7$	I2/a	14.068(2)	4.8600(8) 98.97(1)	8.604(1)	581.07(8)	1D	[23]
$Li_2CuP_2O_7$	C2/c	15.336(1)	4.873(1) 114.80(1)	8.626(2)	585.24(16)	1D	[24]
β-$Na_2CuP_2O_7$	C2/c	14.728(1)	5.698(2) 115.15(1)	8.067(1)	612.88(2)	1D	[25]
$Na_{1.12}Ag_{0.88}CuP_2O_7$	C2/c	15.088(2)	5.641(1) 116.11(1)	8.171(1)	624.48(2)	1D	[26]
Layered structures							
$LiNaCuP_2O_7$	$P2_1/n$	4.988(2)	13.598(4) 92.17(4)	8.294(2)	562.1(3)	2D	This work
α-$Na_2CuP_2O_7$	$P2_1/n$	8.823(3)	13.494(3) 92.77(3)	5.108(2)	607.44(3)	2D	[3]
$LiKCuP_2O_7$	$P2_1/n$	5.065(1)	14.180(2) 90.19(1)	8.473(7)	608.7(5)	2D	This work
$KNaCuP_2O_7$	$P2_1/n$	5.176(3)	13.972(5) 91.34(2)	9.067(3)	655.6 (5)	2D	[12]
$Rb_{0.5}Na_{1.5}CuP_2O_7$	$P2_1/n$	7.811(2)	9.789(3) 104.60(2)	8.636(3)	641.6(3)	2D	This work
$K_2CuP_2O_7$	Pbnm	9.509(4)	14.389(6)	5.276(2)	722.0(6)	2D	[4]
$K_2CuP_2O_7$	$P42_1m$	8.056(2)	-	5.460(11)	354.35 (11)	2D	[27]
$NaCsCuP_2O_7$	$Pmn2_1$	5.147(2)	15.126(3)	9.717(5)	756.5(5)	2D	[19]
Framework structures							
α-$Rb_2CuP_2O_7$	Pmcn	5.183(8)	10.096(1)	15.146(3)	792.5(2)	3D	[28]
β-$Rb_2CuP_2O_7$	Cc	7.002(1)	12.751(3) 110.93(3)	9.773(2)	815.0(3)	3D	[20]
$Cs_2CuP_2O_7$	Cc	7.460(6)	12.973(1) 111.95(1)	9.980(8)	895.8(12)	3D	[29]

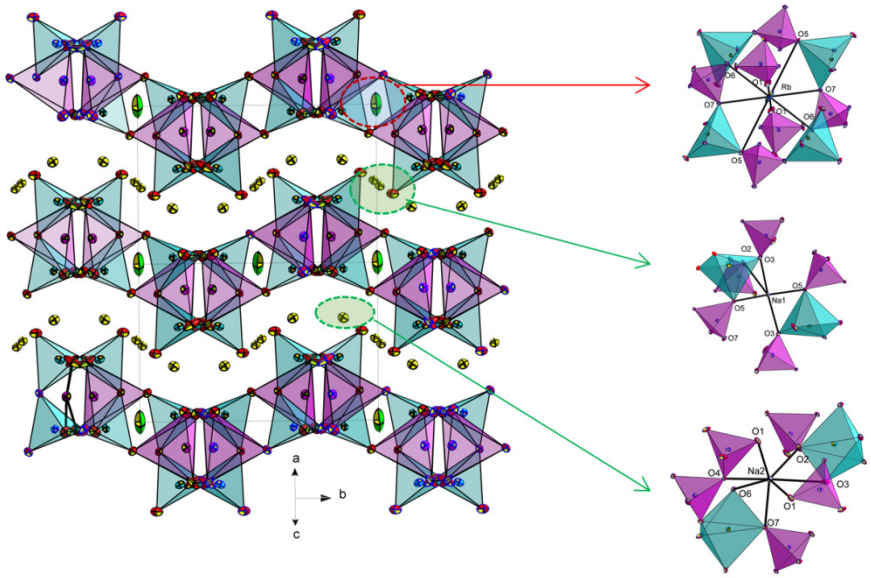

Figure 13. 2-D crystal structure of $Rb_{0.5}Na_{1.5}CuP_2O_7$ projected along [101] direction with details of Rb^+ and Na^+ cations environments.

The character of binding of these structural units depends on the alkali metal cation and leads to various structural patterns. The increasing of the cationic size seems opening the diphosphate bridging angle and its dihedral angle. It contributes to reduce the copper coordination polyhedron distortion leading to slightly regular tetragonal pyramid as confirmed by τ values visible in Table 10. These effects are visible in Figures 12 and 13. Indeed, an attenuation of the interlayer space and the anionic sheets corrugation is clearly observed.

4. Conclusion

Pure phases of $LiNaCuP_2O_7$, $LiKCuP_2O_7$ and $Rb_{0.5}Na_{1.5}CuP_2O_7$ were synthesized by solid state reactions. Single crystal X-ray diffraction investigations revealed that these compounds crystallize in the $P2_1/n$ monoclinic space group and containing nearly eclipsed P_2O_7 diphosphate groups sharing corners with distorted pyramidal square CuO_5 arranged in layered stacking based on two-dimensional anionic network. Small cations prefer crystallographic site located in the interlayer space. Large cations are located in open ellipsoidal cavities situated in the intersection of empty channel delimited by the anionic network. The increasing of the cationic size seems opening the diphosphate bridging angle and its dihedral angle, reducing the copper coordination polyhedron distortion and attenuating the interlayer space and the anionic sheets corrugation. DTA and TGA results revealed the high thermal stability and the absence of any solid state phase transition. The shift observed in the main infrared vibration frequencies of the studied compounds

confirms the crystallographic study. Using the structural data of the three compounds, the cell parameters and the cationic sites occupancies refinement using the Rietveld analysis leads to the same results obtained by the single crystal diffraction study. The same study proofs the high purity of the synthesized samples.

Acknowledgments

We acknowledge the assistance of the staff of the Tunisian Laboratory of Materials and Crystallography for the data collection.

Supplementary data

Further details of the crystal structures investigation are available from the Fachinformationszentrum Karlsruhe, D-76344 Eggenstein-Leopoldshafen, Germany, on quoting the depository number CSD-433889 for the compound $LiKCuP_2O_7$, CSD-433890 for $LiNaCuP_2O_7$ and CSD-434654 for $Rb_{0.5}Na_{1.5}CuP_2O_7$ the names of the authors and the citation of the paper.

Disclosure statement

Conflict of interests: The authors declare that they have no conflict of interest.
Author contributions: All authors contributed equally to this work.
Ethical approval: All ethical guidelines have been adhered.
Sample availability: Samples of the compounds are available from the author.

Funding

Funding for this research was provided by the Tunisian ministry of high education and scientific research.
http://www.mes.tn/

ORCID

Ines Fitouri
http://orcid.org/0000-0001-6428-3909
Habib Boughzala
http://orcid.org/0000-0002-7177-9934

References

[1]. Dupre, N.; Gaubicher, J.; Le Mercrier, T.; Wallez, G.; Angenault, J.; Quarton. M. *Solid State Ionics* **2001**, *140*, 209-221.
[2]. Kurek, P.; Nowinski, J. L.; Jakubowski, W. *Solid State Ionics* **1989**, *36*, 243-246.
[3]. Etheredge, K. M. S.; Hwu, S. J. *Inorg. Chem.* **1995**, *34*, 1495-1499.
[4]. ElMaadi, A.; Boukhari, A.; Holt, E. M. *J. Alloys Compd.* **1995**, *223*, 13-17.
[5]. Prabaharan, S. R. S.; Michael, M. S.; Radhakrishna, S.; Julien, C. *J. Mater. Chem.* **1997**, *7*, 1791-1796.
[6]. Kim, S. W.; Seo, D. H.; Ma, X.; Ceder, G.; Kang, K. *Adv. Energy Mater.* **2012**, *2*, 710-721.
[7]. Coelho, A. A. TOPAS, Version 4.2 (Computer Software), Coelho Software, 2009.
[8]. Sheldrick, G. M. *Acta Cryst. A* **2008**, *64*, 112-122.
[9]. Sheldrick, G. M. *Acta Cryst. C* **2015**, *71*, 3-8.
[10]. Hubschle, C. B.; Sheldrick, G. M.; Dittrich, B. *J. Appl. Cryst.* **2012**, *44*, 1281-1284.
[11]. ICSD 2017. Inorganic Crystal Structure Database. FIZ-Karlsruhe, Germany.
[12]. Fitouri, I.; Boughzala H. *Acta Cryst. E* **2018**, *74*, 109-112.
[13]. Brown, I. D. *Phys. Chem. Minerals* **1987**, *15*, 30-34.
[14]. Hoppe, R.; Voigt, S.; Glaum, H.; Kissel, J.; Muller, H. P.; Bernet, K. J. *Less-Common Met.* **1989**, *156*, 105-122.
[15]. Nespolo. M. CHARDT-IT, A Program to Compute Charge Distributions and Bond Valences in Non-Molecular Crystalline Structures, LCM3 B, University Henri Poincare Nancy I, France, 2001.
[16]. Nespolo, M.; Eon, J. G. *Acta Cryst. B* **2001**, *57*, 652-664.
[17]. Brandenburg, K. DIAMOND. 3. 1, Crystal Impact GbR, Bonn, Germany, 2008.
[18]. Toby, B. H. EXPGUI, *J. Appl. Cryst.* **2001**, *34*, 210-213.
[19]. Chernyatieva, A. P.; Krivovichev, S. V.; Spiridonova, D. V. Proceedings of the XX Russian Conference of Young Scientists in Memory of the Corresponding Member of the Academy of Sciences of the USSR, K. O. Kratts, 2009.
[20]. Shvanskaya, L. V.; Yakubovich, O. V.; Urusov, V. S. *Dokl. Phys. Chem.* **2012**, *442*, 19-26.
[21]. Addison, A. W.; Rao, T. N.; Reedijk, J.; Van Rijn, J.; Verschoor, G. C. *J. Chem. Soc. Dalton Trans.* **1984**, *3*, 1349-1356.
[22]. Bouhassine, M. A.; Boughzala, H. *Acta Cryst. E* **2014**, *70*, i6-i6.
[23]. Spirlet, M. R.; Rebizant, J.; Liegeois-Duyckaerts, M. *Acta Cryst. C* **1993**, *49*, 209-211.
[24]. Gopalakrishna, G. S.; Mahesh, M. J.; Ashamanjari, K. G.; Prasad, J. S. *Mater. Res. Bull.* **2008**, *43*, 1171-1178.
[25]. Erragh, F.; Boukhari, A.; Abraham, F.; Elouadi, B. *J. Solid State Chem.* **1995**, *120*, 23-31
[26]. Bennazha, J.; Boukhari, A.; Holt, E. M. *Acta Cryst. C* **2002**, *58*, 87-89.
[27]. Keates, A. C.; Wang, Q.; Weller, M. T. J. *Solid State Chem.* **2014**, *210*, 10-14.
[28]. Chernyatieva, A. P.; Krivovichev, S. V.; Spiridonova, D. V. Book of Abstracts VI International Conference "Inorganic Materials" Dresden: Elsevier, 2008, 3-143.
[29]. Mannasova, A. A.; Chernyatieva, A. P.; Krivovichev, S. V. *Z. Kristallogr.* **2016**, *231*, 65-69.